The Regional Nature of Aerodynamic Jump

by Mark Bundy

19990304 008

Army Research Laboratory

Aberdeen Proving Ground, MD 21005-5066

The Regional Nature of Aerodynamic Jump

Mark Bundy
Weapons and Materials Research Directorate, ARL

Abstract

It is shown that aerodynamic jump for a nonspinning kinetic energy penetrator is neither a point change in direction, nor a curving change that takes place over a domain of infinite extent, as conventional definitions may infer. Rather, with the aid of an alternative kinematical definition, it is shown that aerodynamic jump for such a projectile is a localized redirection of the center-of-gravity motion, caused by the force of lift due to yaw over the relatively short region from entry into free flight until the yaw reaches its first maximum. A rigorous proof of this statement is provided, but the primary objective of this report is to provide answers to the questions: What is aerodynamic jump, what does it mean, and what aspects of the flight trajectory does it refer to, or account for?

REPORT DOCUMENTATION PAGE

Public reporting burden for this collection of information is estimated to average 1 hour per response, including the time for reviewing instructions, searching existing data sources, gathering and maintaining the data needed, and completing and reviewing the collection of information. Send comments regarding this burden estimate or any other aspect of this collection of information, including suggestions for reducing this burden, to Washington Headquarters Services, Directorate for Information Operations and Reports, 1215 Jefferson Davis Highway, Suite 1204, Arlington, VA 22202-4302, and to the Office of Management and Budget, Paperwork Reduction Project(0704-0188), Washington, DC 20503.

1. AGENCY USE ONLY *(Leave blank)*	2. REPORT DATE January 1999	3. REPORT TYPE AND DATES COVERED Final, Nov 97 - Nov 98

4. TITLE AND SUBTITLE The Regional Nature of Aerodynamic Jump	5. FUNDING NUMBERS 1L162618AH80
6. AUTHOR(S) Mark Bundy	

7. PERFORMING ORGANIZATION NAME(S) AND ADDRESS(ES) U.S. Army Research Laboratory ATTN: AMSRL-WM-BC Aberdeen Proving Ground, MD 21005-5066	8. PERFORMING ORGANIZATION REPORT NUMBER ARL-TR-1872

9. SPONSORING/MONITORING AGENCY NAMES(S) AND ADDRESS(ES)	10.SPONSORING/MONITORING AGENCY REPORT NUMBER

11. SUPPLEMENTARY NOTES

12a. DISTRIBUTION/AVAILABILITY STATEMENT Approved for public release; distribution is unlimited.	12b. DISTRIBUTION CODE

13. ABSTRACT *(Maximum 200 words)*

It is shown that aerodynamic jump for a nonspinning kinetic energy penetrator is neither a point change in direction, nor a curving change that takes place over a domain of infinite extent, as conventional definitions may infer. Rather, with the aid of an alternate kinematical definition, it is shown that aerodynamic jump for such a projectile is a localized redirection of the center-of-gravity motion, caused by the force of lift due to yaw over the relatively short region from entry into free flight until the yaw reaches its first maximum. A rigorous proof of this statement is provided, but the primary objective of this report is to provide answers to the questions: What is aerodynamic jump, what does it mean, and what aspects of the flight trajectory does it refer to, or account for?

14. SUBJECT TERMS aerodynamic jump, swerve axis, first maximum yaw, origin of free flight	15. NUMBER OF PAGES 52
	16. PRICE CODE

17. SECURITY CLASSIFICATION OF REPORT UNCLASSIFIED	18. SECURITY CLASSIFICATION OF THIS PAGE UNCLASSIFIED	19. SECURITY CLASSIFICATION OF ABSTRACT UNCLASSIFIED	20. LIMITATION OF ABSTRACT UL

INTENTIONALLY LEFT BLANK

TABLE OF CONTENTS

INTENTIONALLY LEFT BLANK

ACKNOWLEDGMENTS

The author would like to thank Dr. Peter Plostins (U.S. Army Research Laboratory) for serving as technical reviewer of this document.

INTENTIONALLY LEFT BLANK

LIST OF FIGURES

INTENTIONALLY LEFT BLANK

1. INTRODUCTION

The motion of a projectile can be separated into two general regions: the free-flight, FF, region and the launch-disturbance, LD, region (prior to FF). For instance, if the projectile is a saboted long rod (or, kinetic energy, KE) penetrator, then the LD region begins in-bore and extends downrange to the point where shock waves from the discarding sabot petals no longer interact with the rod. The end of the LD region marks the beginning of the FF region, where the phenomenon known as aerodynamic jump (AJ) occurs. The KE penetrator is chosen to facilitate the ensuing discussion and illustrations on the subject of AJ.

Although AJ occurs in the FF region, its magnitude is influenced by events that take place in the LD region. Hence, a brief discussion of LD effects is in order. A KE projectile consists of a long rod with an aerodynamically shaped nose and stabilizing tail fins. The high mass-density, sub-caliber rod is held centered in the gun bore by a low mass-density, full-caliber sabot. The rod can undergo small, lateral, center-of-gravity (cg) displacements and rotations while being propelled longitudinally down the bore. Such in-bore motion permits the projectile cg to exit the barrel with a velocity vector oriented at an angle $\angle CG$ with respect to the instantaneous bore axis. In addition to the rod moving relative to the bore axis, the barrel itself can be moving. Thus, the rod can be launched with the instantaneous pointing angle of the bore axis, $\angle PA$, different from the original muzzle sight line. Furthermore, the instantaneous bore axis can have a lateral (crossing) velocity that is transferred to the projectile cg motion. The angular change in the projectile cg velocity due to this barrel crossing motion is denoted by $\angle CV$. Outside the gun, it is possible for asymmetric sabot discard to create uneven mechanical and aerodynamic forces on the rod that add yet another transverse cg velocity component, and redirection angle, $\angle SD$. The net effect of these four pre-free-flight LDs can give the projectile cg a cumulative transverse deflection angle, $\angle LD = \angle CG + \angle PA + \angle CV + \angle SD$, at the point

1

where it enters FF, Figure 1. Bornstein et al. (1988) outlines techniques to measure these LD components.
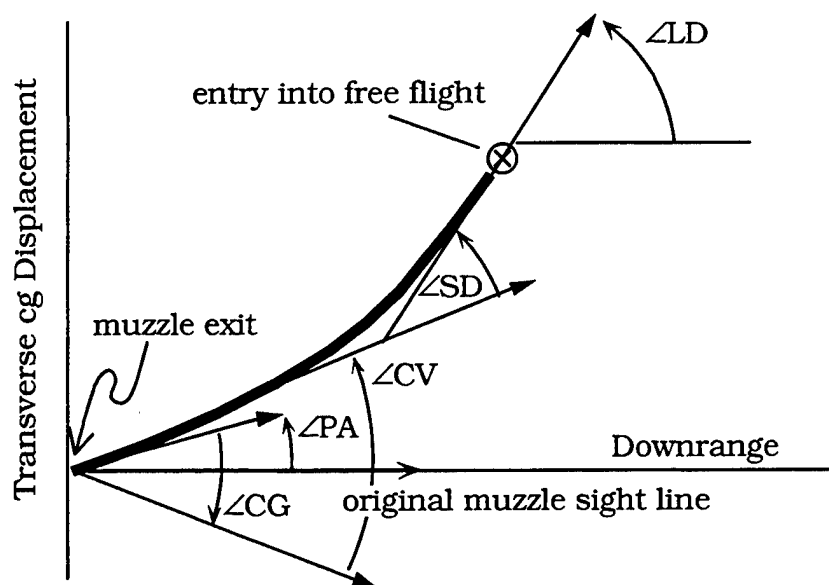
Figure 1. Hypothetical Planar CG Motion of a KE Rod Caused by Launch Disturbances.

After traveling through the LD region, the KE rod enters FF. The motion of the projectile in FF is influenced by time-dependent side forces that cause the projectile cg to oscillate (swerve) about a mean FF path (swerve axis) as it travels to the target, Figure 2. For a typical KE rod (which is statically stable, near-symmetric, and virtually nonrolling), the swerve curve can be approximated by a damped sine wave in both the vertical and horizontal directions.
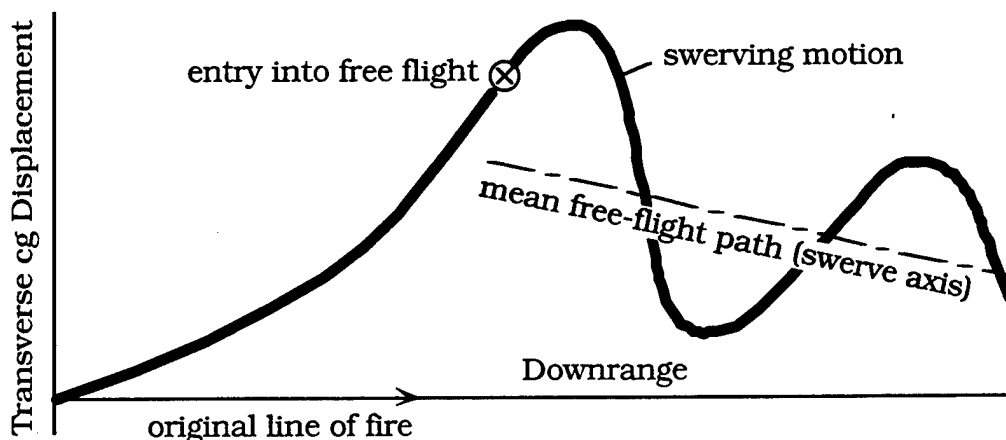
Figure 2. Transition of CG Trajectory Into Free Flight.

2

As the trajectory of Figure 2 is extended to a distant target, the swerve amplitude decays to near zero and the point of impact lies close to the axis of swerve symmetry, Figure 3. (Note, the effects of gravity and the Coriolis force on the trajectory are not included in this discussion because they are not aerodynamic in nature; if warranted, their influence can simply be superimposed on the swerve motion.)
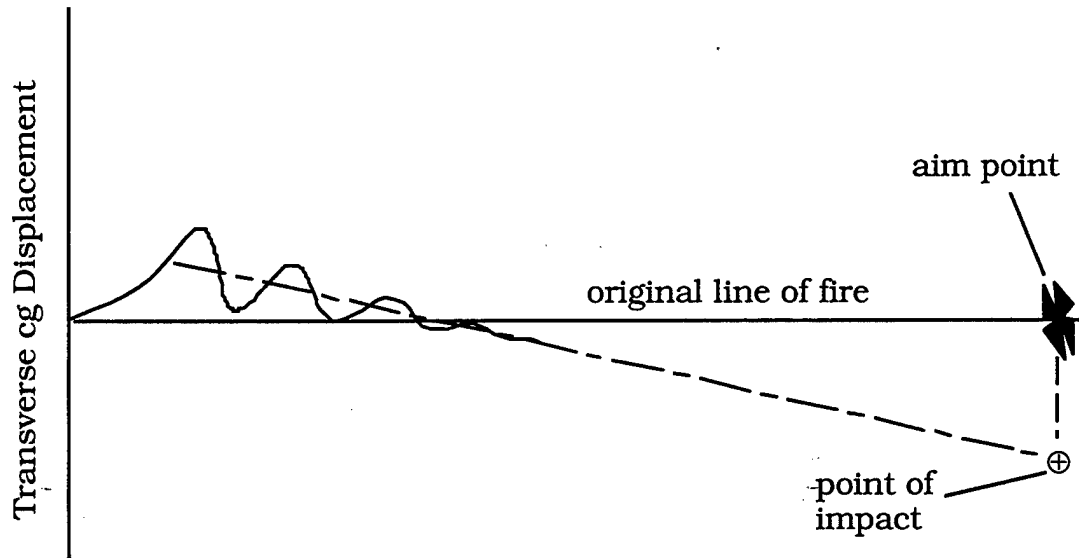
Figure 3. Hypothetical CG Trajectory Extended to the Target.

Thus, the axis of swerve symmetry has special significance because it is closely aligned with the point of impact on a distant target. As indicated by Figures 2 and 3, the swerve axis can be, and most often is, different from the direction given to the projectile cg as it leaves the LD region. This change in direction is caused by FF aerodynamic side forces. The term "aerodynamic jump," AJ, is used to quantify this change in direction.

One of the earliest descriptions of AJ was given by Murphy (1957), stating that AJ is "the angle between the bore sightline and the 'average' trajectory when other contributors to jump are neglected." Although this definition describes AJ as an angle, it is actually the tangent of the described angle. However, for small angles (typical for AJ), the angle and its tangent are nearly one and the same. Neglecting other contributors to jump, as per Murphy

(1957), would mean setting, or assuming, $\angle LD$ = 0 in the previous discussion. In this case, Figure 3 would transform into Figure 4.
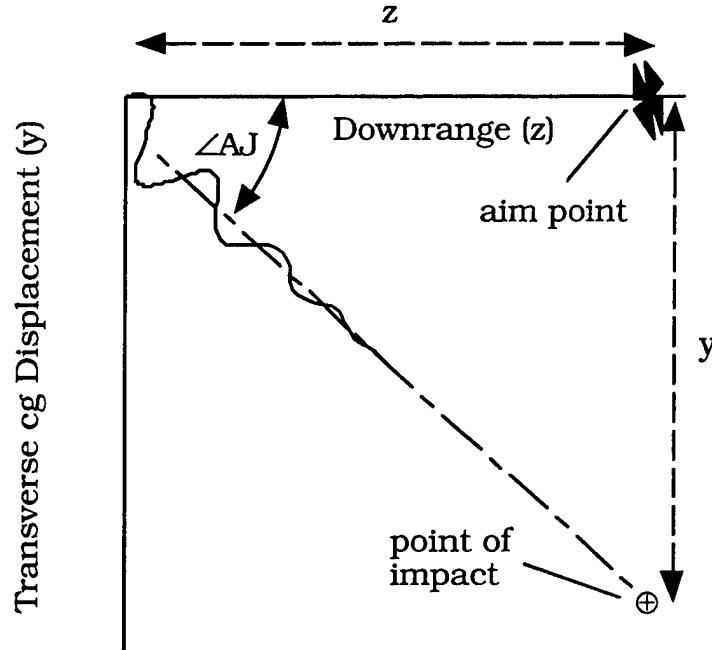
Figure 4. Geometrical View of $\angle AJ$, Neglecting $\angle LD$.

From Figure 4, when the FF trajectory approaches infinity, AJ and $\angle AJ$ can be defined by

$$AJ \ = \ \lim_{z\to\infty}\left[\frac{y}{z}\right] \ ; \quad \angle AJ \ = \ \tan^{-1}\{AJ\} \underset{AJ,\ \angle AJ\,<<\,1}{\approx} AJ \ , \tag{1}$$

where y represents the transverse cg displacement and z represents the longitudinal, or downrange, displacement. (Note, for later reference, the sign convention for the direction of positive y in Equation 1 will determine the sign convention for positive AJ.) Both Murphy (1957) and Murphy and Bradley (1959) begin their discussion of AJ based on Equation 1. A more inclusive expression for AJ, one that does not neglect "other contributors to jump," is put forth later by Murphy (1963); this more general definition states:[*]

---

[*] Equation 2, here, is actually the single-plane equivalent of combining Murphy's (1963) Equations 9.8 and 10.1, with gravitational and Coriolis effects neglected.

4

$$AJ = \lim_{z \to \infty} \left[\frac{y - y_0}{z - z_0} \right] - \frac{dy}{dz} \bigg|_{z_0} \quad ;$$

$$\angle AJ \approx \lim_{z \to \infty} \left[\frac{y - y_0}{z - z_0} \right] - \frac{dy}{dz} \bigg|_{z_0} \quad , \qquad (2)$$

$$\lim_{z \to \infty} \left[\frac{y - y_0}{z - z_0} \right], \frac{dy}{dz} \bigg|_{z_0} \ll 1$$

where y_0 is the transverse cg displacement and $dy/dz\big|_{z_0}$ is the tangent to the cg displacement, both at the origin of FF. Figure 5 (an annotated rendering of Figure 3) gives the geometrical interpretation of Equation 2.
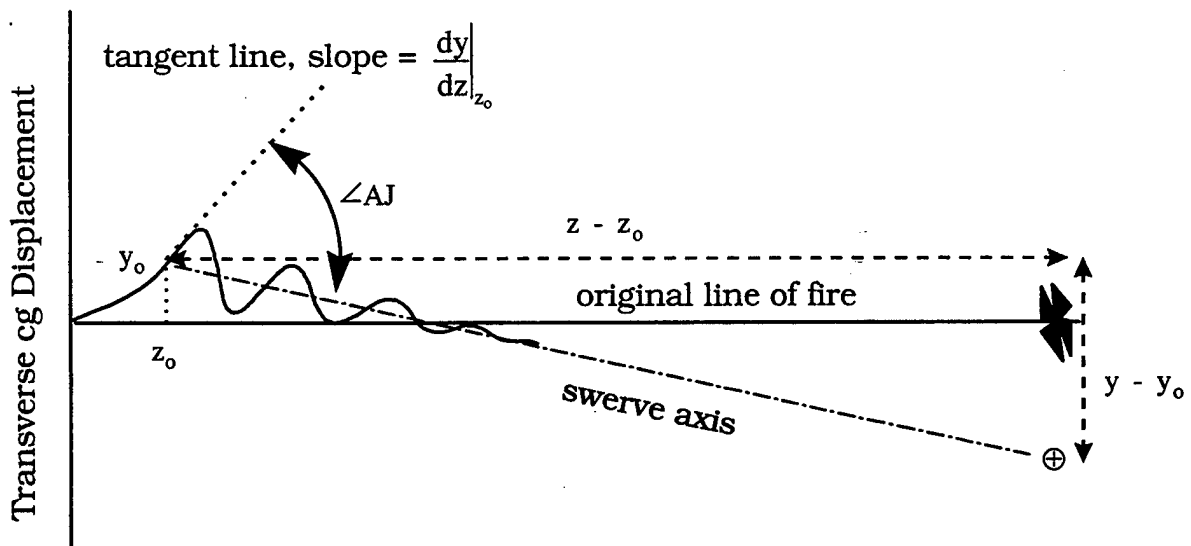
Figure 5. Geometrical Interpretation of Equation 2.

Equations 1 and 2 are kinematical definitions for AJ. Their more familiar dynamical counterparts are derived from them by solving, then substituting for y and z based on the equations of motion (as done in section 5 of this report). Although the dynamical expressions for AJ may be more useful in practical applications, the simple geometry-based definitions of Equations 1 and 2 are the most helpful for those seeking to visualize the effect of AJ on the cg trajectory. However, because Equations 1 and 2 call upon the limit as the trajectory approaches infinity, some may erroneously infer from this that AJ is an effect that "accumulates" with downrange distance. In other words,

they may wrongly assume from these infinity-based definitions that it takes a near-infinite amount of space to establish the AJ. The purpose of this report is to dispel any such notions by showing that the bending of the "average" trajectory, referred to as AJ, is due to aerodynamic forces acting over a relatively short segment of the FF trajectory. This will be done, in triplicate, by first giving an alternative geometry-based, or kinematical definition for AJ. Then, a physically sound explanation, supporting this definition, is given. And finally, the theoretical consequences promulgated from the alternative kinematic definition are shown to produce the same dynamical expression for AJ as that derived from Equations 1 and 2.

2. AN ALTERNATIVE KINEMATICAL DEFINITION FOR AJ

To some, it may already be obvious (from Figures 4 or 5) that because $\angle$AJ is the angle between two straight lines (viz., the tangent to the cg curve at z_0, y_0, and the swerve axis), it is fixed in space as soon as these lines are established. Therefore, it will not change with, nor depend upon, downrange distance after some point—but where is this terminal point? If the swerve axis is exactly aligned with the cg tangent at y_0, z_0, then the point in question is precisely at the origin of FF, in which case, however, $\angle$AJ = 0. On the other hand, if $\angle$AJ is nonzero, then the swerve axis will be established over a nonzero, but finite region of the trajectory, as discussed next.

From Equation 2 and Figure 5, $\angle$AJ is the angular change between the tangent to the cg trajectory at the end of the LD region and the axis of swerve symmetry. Since the tangent to the cg trajectory at y_0, z_0 is oriented at $\angle$LD with respect to the original line of fire, an equally suitable descriptioon of Equation 2 is depicted in Figure 6.

6
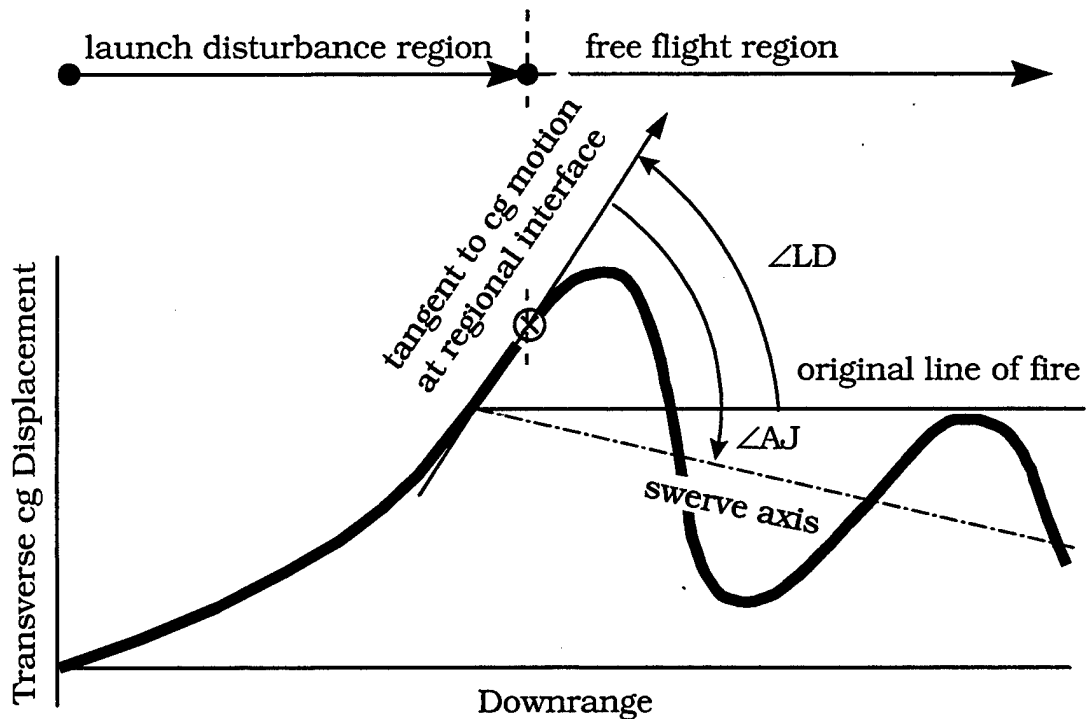
Figure 6. Alternative Description of $\angle$AJ.

As shown in Figure 7 (and formally proven in Appendix A), the tangent to the swerve curve at any of the local maxima (positive or negative with respect to the swerve axis) will be parallel to the swerve axis. Hence, $\angle$AJ can also be defined as the angular difference between the tangent to the swerve curve at the origin of FF and the tangent to the swerve curve at the first (or second, or third, etc.) local maximum in the swerving motion. In equation form,

$$\angle\text{AJ} = \tan^{-1}\left\{\frac{dy}{dz}\bigg|_{z_{\text{swerve maxima}}}\right\} - \tan^{-1}\left\{\frac{dy}{dz}\bigg|_{z_{\text{origin of free flight}}}\right\}$$

$$\approx \frac{dy}{dz}\bigg|_{z_{\text{swerve maxima}}} - \frac{dy}{dz}\bigg|_{z_{\text{origin of free flight}}}$$

(3)

where the subscripts identify the locations at which the derivatives are to be evaluated.
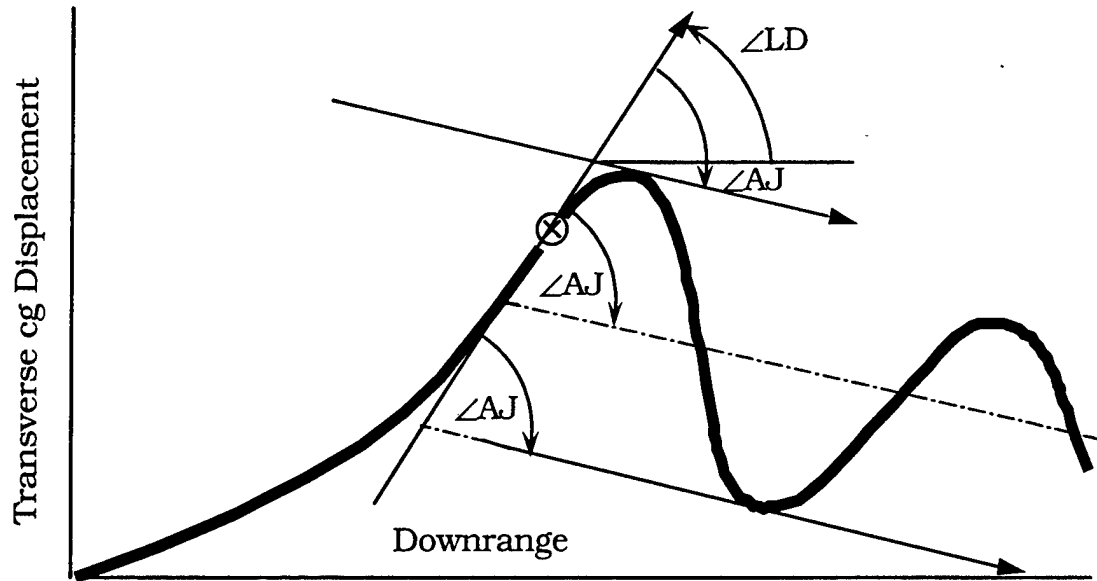
Figure 7.   Alternative Geometrical Definitions for $\angle$AJ.

Even though $\angle$AJ can be defined using the tangent line at any of the local maxima, as depicted in Figure 7, it is clear that the minimum distance needed to establish the orientation of the swerve axis is the distance to the first swerve maxima, z_1. Thereafter, the cg motion simply oscillates back and forth about this axis, albeit with damped amplitude.

Unlike Figure 7, the swerve axes in Figures 8a and 8b are nearly parallel with the LD direction. Hence, the angle between the swerve axis and the LD direction ($\angle$AJ) is smaller than that shown in Figure 7. It is also apparent that the distance between the origin of free fight, z_0, and the first swerve maximum, z_1, is relatively small in Figure 8a (at least in comparison with the wavelength of the swerve curve, λ), but relatively large in Figure 8b. Contrasting the larger $\angle$AJ of Figure 7 with that of Figures 8a and 8b, it can be deduced that the largest $\angle$AJ will occur when $z_1 - z_0 = \lambda/4$. In fact, if the swerve curve is approximated by a sine wave of the form $y = A\sin(2\pi[z-z_0]/\lambda)$, at least for the first cycle, then, from Equation 3, the maximum $\angle$AJ would be given by

8

$$\left| \angle AJ_{max} \right| = \left| \frac{d\left\{ y = A \sin\left(\frac{2\pi[z-z_0]}{\lambda} \right) \right\}}{dz} \right|_{z_1 = z_0 + \lambda/4} - \left. \frac{d\left\{ y = A \sin\left(\frac{2\pi[z-z_0]}{\lambda} \right) \right\}}{dz} \right|_{z_0} \right| \quad . \quad (4)$$

$$= \frac{A\,2\pi}{\lambda}$$

To appreciate the significance of Equation 4, Figure 9 illustrates how $\angle AJ_{max}$ varies with A and λ, for two cases where y conforms to $A\sin(2\pi[z-z_0]/\lambda)$. From the depiction, a larger A and smaller λ produce a larger $\angle AJ_{max}$. For large-caliber guns, A may be on the order of several millimeters, whereas λ is on the order of tens of meters; hence, $\angle AJ_{max}$, from Equation 4, will be small—on the order of milliradians.

Figures 7–9, and the discussions thereabout, illustrate that the axis of swerve symmetry is fixed in space by the time the rod reaches its first swerve maximum, as stated in Equation 3. They also provide visible examples that support the contention that it is not necessary to take the swerving motion to infinity, as called for in Equations 1 and 2, in order to establish the swerve axis. A more rigorous, analytical, proof of these assertions is given in section 5.

9
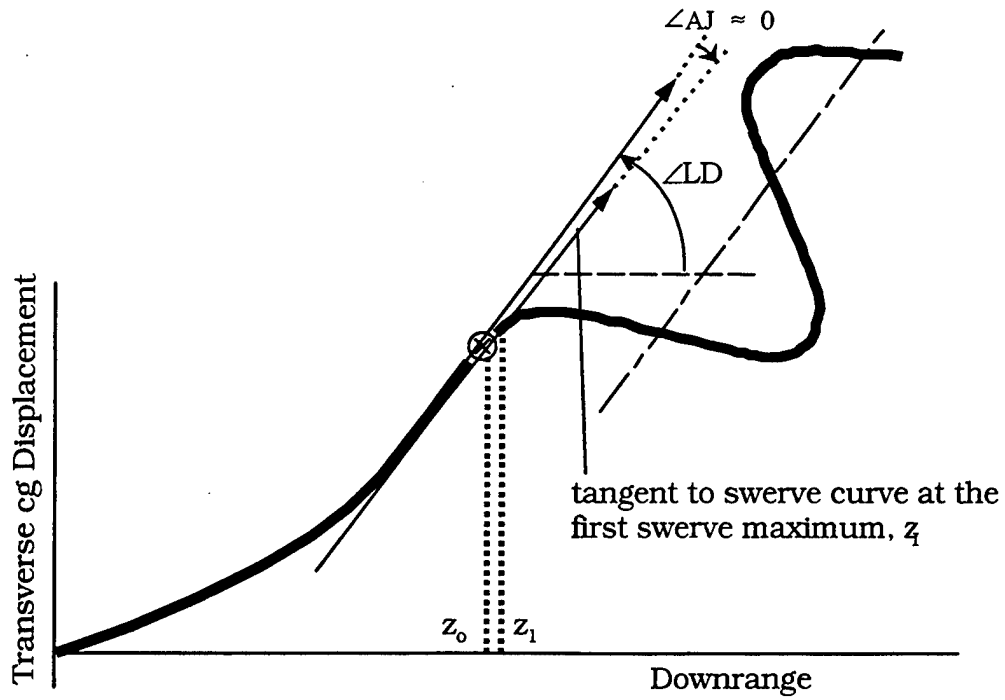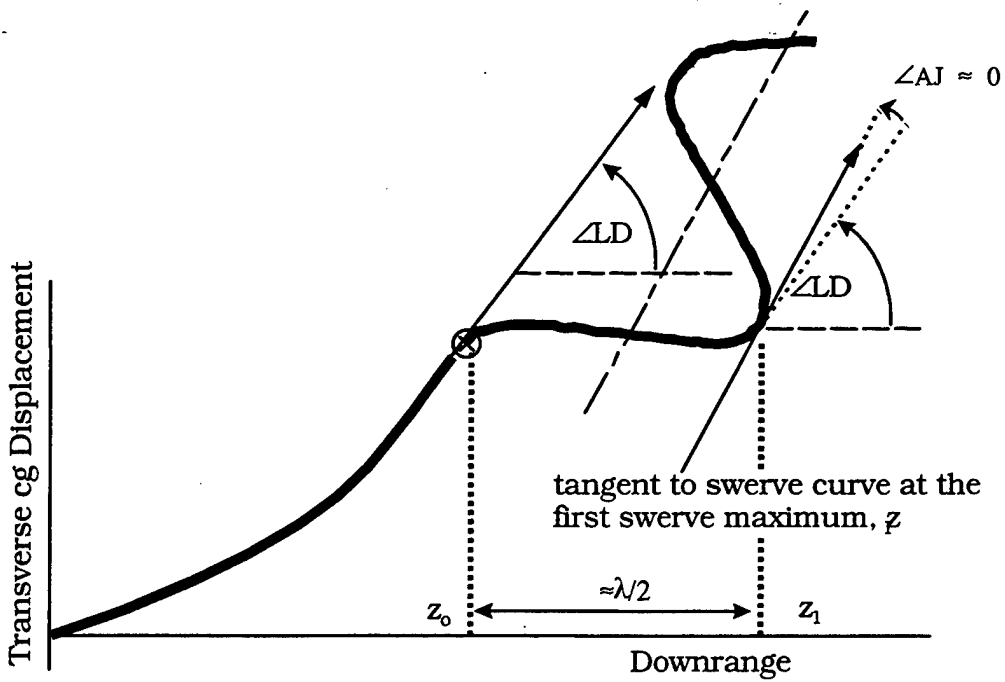
Figure 8. The Influence of Initial (Swerve) Conditions on AJ, a) Entry Into FF at $z_o \approx z_1$, and b) Entry Into FF at $z_o \approx z_1 - \lambda/2$.

10
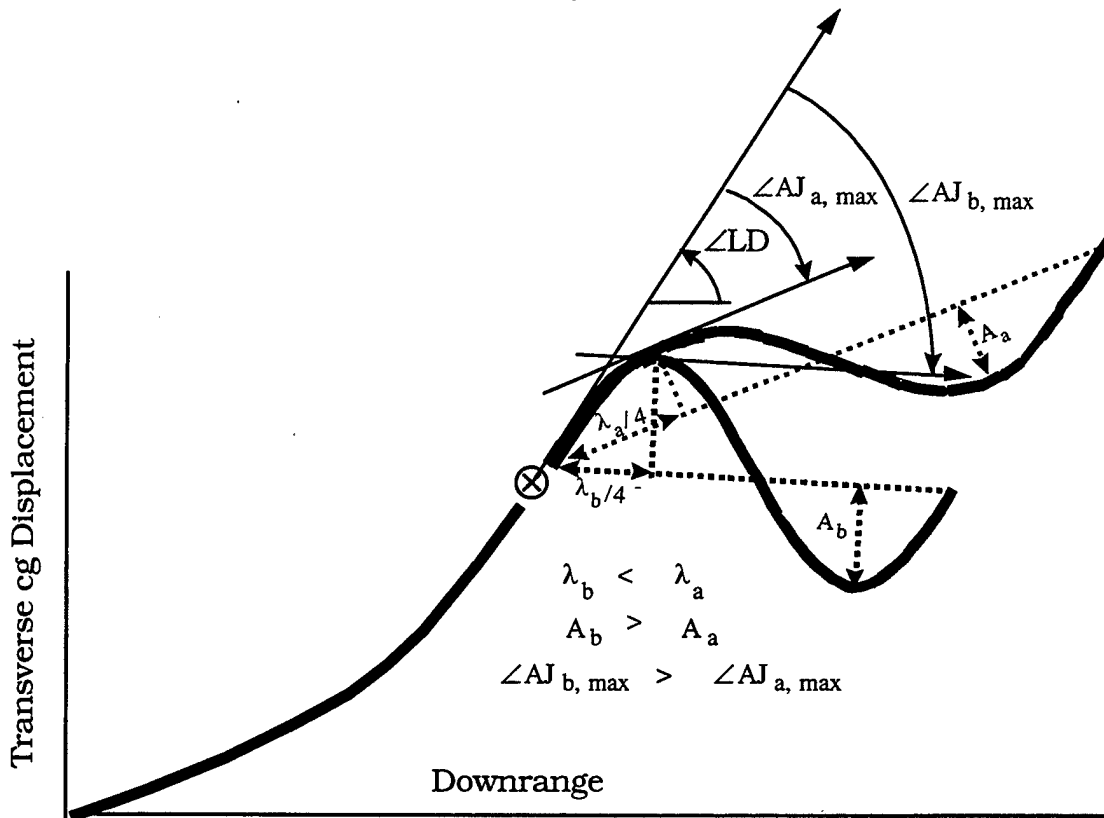
Figure 9. Depiction of Variation in $\angle AJ_{max}$ With Amplitude and Wavelength of the Swerve Curve

Thus far, the subject of AJ has been limited to a geometrical discussion of the projectile cg path. However, geometry alone does not provide physical insight into how the cg path can turn away from the LD direction after the rod enters FF. Section 3 constructs a physical model that identifies the aerodynamic force that causes such a change in direction to occur.

3. A PHYSICAL EXPLANATION FOR AJ

A KE penetrator is also called a long-rod penetrator, conveying the fact that its fundamental shape is a high length-to-diameter ratio cylinder. It is fin stabilized, with only a small roll rate (assumed here to be zero). There are two fundamental aerodynamic forces on such a rod, one is drag, $\vec{D}$, and the

11

other is lift $\bar{L}$. The combination of drag and lift produces a resultant force, $\bar{R}$ $(=\bar{L}+\bar{D})$, acting at the center of pressure, cp, as shown in Figure 10. The drag force is opposite in direction to $\bar{u}$, while the lift force is perpendicular $\bar{u}$. However, lift is only nonzero if the angle of yaw (α) between the symmetric rod axis and $\bar{u}$ is nonzero. Since the Magnus force is absent for a nonrolling projectile, lift is the only aerodynamic force that is capable of producing the type of lateral cg motion needed to explain AJ.
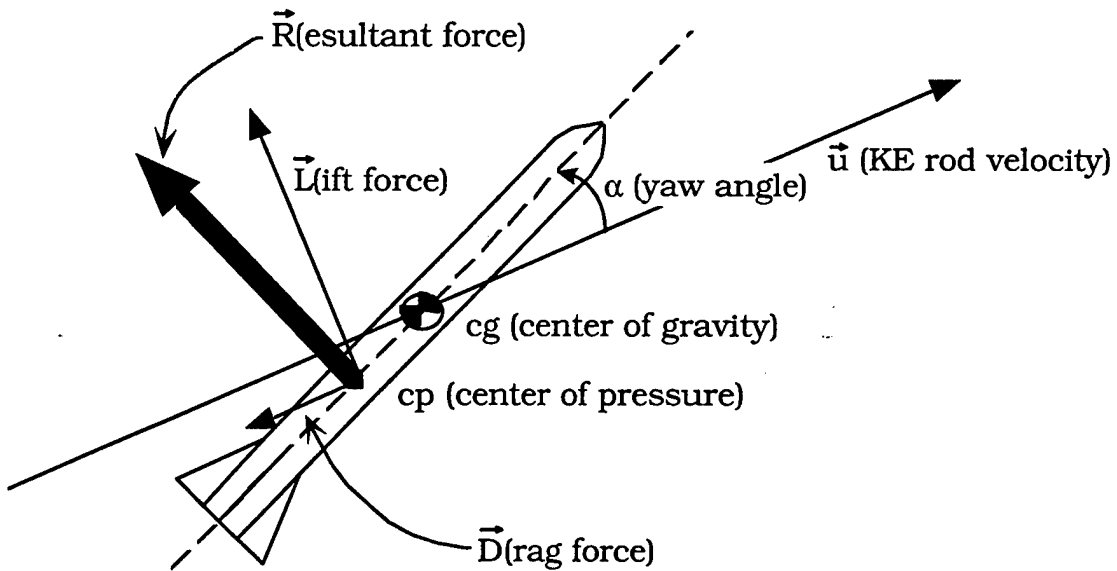
Figure 10. Illustration of the Lift and Drag Force Directions, as Well as the CG and CP Locations for a Typical KE Rod.

In order to understand how the lift force can, in fact, account for AJ, it is necessary to discuss the factors that control α (thereby controlling lift). By Newton's second law for angular motion, yaw will be controlled by the aerodynamic moment, $\bar{M}$, that acts about the projectile cg. For a properly designed nonspinning KE rod, $\bar{M}$ will tend to decrease α, i.e., tend to align the rod axis with $\bar{u}$. Consider then, what happens when such a KE penetrator enters FF.

12

Suppose, as shown in Figure 11 (which displays the same cg motion as Figures 2, 3, 5, 6, and 7), the transverse component of the cg velocity is positive at the point where the rod enters FF, i.e., $\dot{y}_o > 0$ at y_o, z_o (attributed to a particular combination of LD effects, e.g., Figure 1). Furthermore, assume that at entry into FF, the KE rod has a negative initial yaw, $\alpha_o < 0$ (represented, here, as a clockwise rotation of the rod axis below the impinging airstream in Figure 11) and a negative initial yawing rate, $\dot{\alpha}_o < 0$ (given a clockwise arrow). Under these conditions, the flow of air will create an initial lift force with a negative-y component (reducing $\dot{y}$), and a negative-x directed moment $\vec{M}$, which (in lieu of being out of the page in Figure 11) is depicted as a counterclockwise arrow. Eventually, the negative lift force will turn the cg motion around, so that $\dot{y} < 0$. Likewise, the counterclockwise $\vec{M}$ will eventually turn the angular motion around, changing the yaw rate from its initial negative value (clockwise) to a positive one (counterclockwise), $\dot{\alpha} > 0$. These changes in direction occur around the first local maximum in the swerve-curve. In fact, it is shown in Appendix B that the yaw angle will be at its maximum at the local swerve maximum.
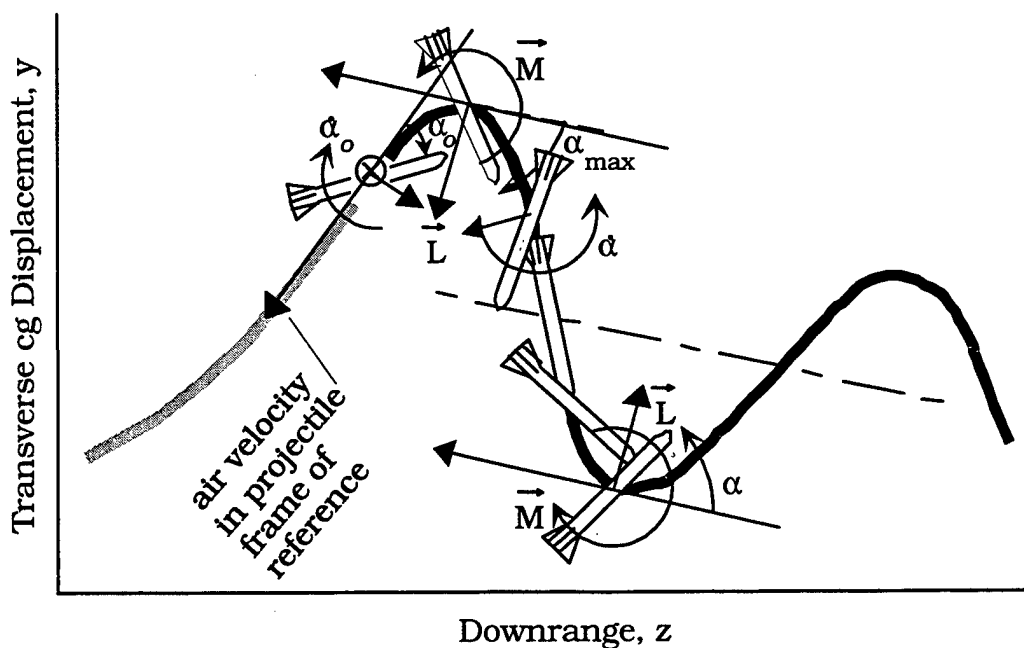

Figure 11. Angular Orientations of a KE Rod Consistent With the CG Trajectory of Figures 2, 3, 5, 6 and 7.

13

After bringing the clockwise rotation to a halt at its maximum (negative) yaw angle, α_{max}, the counterclockwise moment in the first half cycle reverses the yaw rotation and eventually brings α to zero. This occurs when the y component of the rod's cg crosses the swerve axis, as pictured. Throughout this period of time, the lift force remains negative; thus, the rod cg will enter the second half cycle of the swerve motion with negative-y momentum. Similarly, the counterclockwise angular momentum rotates α past zero at the swerve axis, giving the rod a positive yaw in the second half cycle. However, when α becomes positive, it generates a positive lift force and a positive-x directed (into the page) clockwise moment $\overline{M}$ that opposes further increases in α, as depicted in Figure 11. Such projectiles are said to be statically stable, which simply means that if the projectile is held statically at some nonzero yaw angle, and then released (as might be the case in a wind tunnel experiment), the yaw will decrease.

Hence, the conditions present in the first half cycle of FF are exactly reversed in the second half of the swerve cycle. Therefore, with the exception of a reversal in directions, the explanation for events in the second half cycle will be identical to that which accounted for the first half cycle motion. In a like manner, each cycle in the swerving motion of the KE rod cg can be understood as resulting from the oscillation in lift created by a periodic motion in yaw. (Further discussion on the phase relationships between yaw, yaw rate, transverse displacement, and transverse velocity can be found in Appendix B.)

Although the previous arguments infer that the change in cg direction between the point of entry into FF and the first maximum yaw ($\equiv \angle AJ$) is attributable to the force of lift due to yaw over this region, the dependence of $\angle AJ$ on initial conditions cannot be fully appreciated until Figure 8 is compared with Figure 7 in the following manner.

Figure 12, like its counterpart in Figure 11, displays a set of initial and subsequent FF conditions that are consistent with the cg motion of Figure 8.

Specifically, as illustrated, the initial yaw angle of the rod as it enters FF is near its maximum (albeit negative) value, $\alpha_0 \approx \alpha_{max}$, therefore, the initial yaw rate is near zero, $\dot{\alpha}_0 \approx 0$. Furthermore, since the initial yaw is negative, $\overline{L}$ is initially directed toward the swerve axis and $\overline{M}$ is initially in the negative-x direction (out of the page). These are exactly the same conditions that were present at the first local maximum in the swerving motion of Figure 11. Therefore, from the point of first maximum yaw onward, the lift force affecting the cg motion of Figure 12 is exactly the same as that governing the cg motion of Figure 11. Yet, the direction of the swerve axis is seen to be noticeably different, in particular, the $\angle$AJ is noticeably different. The significance of this observation is the sum and substance of this report. That is, since the aerodynamic force on the KE rod is essentially the same from the first maximum onward in both Figures 11 and 12, yet $\angle$AJ is significantly different in the two figures, it must be the case that $\angle$AJ is due to differences in the lift force prior to the first maximum yaw. Once again, implicating that AJ is a regional effect, occurring from the point of entry into FF up to the point of first maximum yaw.
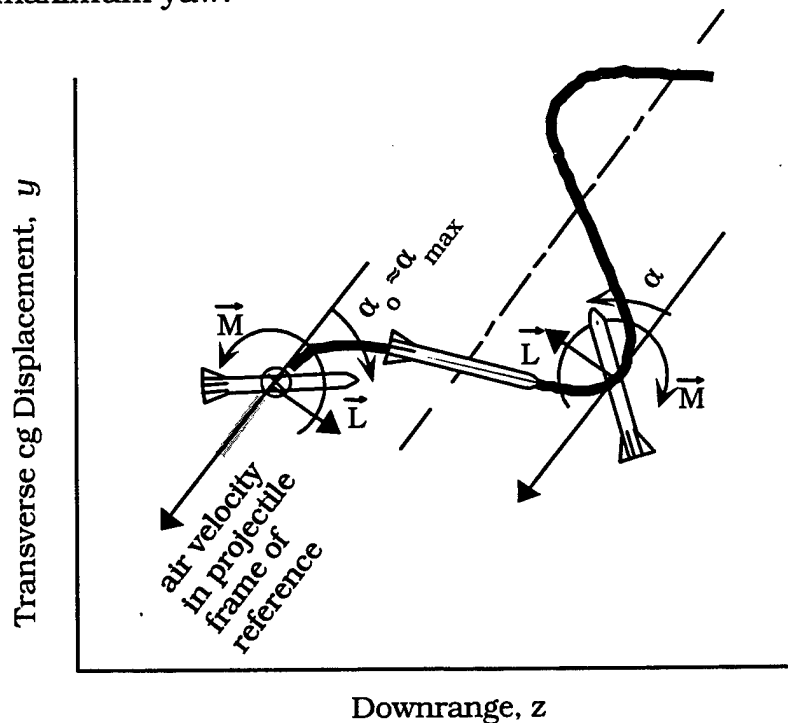

Figure 12. Angular Orientations of a KE Rod Consistent With the CG Trajectory of Figure 7.

15

Ultimately, differences in the lift force, more correctly, differences in the integrated lift force, up to the point of first maximum yaw are governed by differences in the initial conditions. That is, in both Figures 11 and 12, the rod enters FF with an appreciable initial yaw angle, but only in the case of Figure 11 was the initial yaw rate, $\dot{\alpha}_o$, notably different than zero. Comparing this with the observation that $\angle AJ$ was only substantial for the initial conditions of Figure 11, it can be deduced that $\angle AJ$ is not dependent upon the initial yaw angle, but rather, it is dependent on the initial yaw rate. It is shown in section 5 that, indeed, the mathematical expression for $\angle AJ$ of a nonspinning KE rod depends on the initial yaw rate, not yaw. (Bear in mind, for the more general case of a spinning projectile, $\angle AJ$ depends on both yaw and yaw rate.)

Based on the kinematical development of section 2, and the physical model of section 3, it is now a simple matter to derive a dynamical expression for AJ. However, before such an expression can be formulated, it is necessary to develop expressions for the basic aerodynamic forces and moments.

4. BASIC AERODYNAMIC FORCES AND MOMENTS ACTING ON A NONSPINNING KE PENETRATOR

The force of friction, drag, on the projectile is commonly expressed as

$$\bar{D} = -\frac{1}{2} C_D \rho A |\bar{u}| \bar{u} , \tag{5}$$

where C_D is called the drag coefficient, ρ is the air density, A is the cross-sectional area of the projectile, and, by virtue of the minus sign, drag is in the direction opposite $\bar{u}$, the cg velocity vector (Figure 10). For small yaw (e.g., $\alpha < 5°$), typical of KE rods, C_D can be considered a constant.

16

The expression for lift is conventionally written as

$$\vec{L} = \frac{1}{2} C_L \rho A |\vec{u}|^2 \hat{L} , \tag{6}$$

where C_L is referred to as the lift coefficient. The unit-vector direction of the lift force, $\hat{L}$, is perpendicular to the drag force and is in the yaw plane.

Here, yaw is the vertical(z–y)-plane angle, α, between the projectile's tail-to-nose axis and the tangent to its trajectory (or, equally suitable, $\vec{u}$). As typical, it is assumed here that a positive α means the nose of projectile is above $\vec{u}$. A projectile flying at zero yaw has no lift, whereas one having a positive α generates a positive lift (the case depicted in Figure 10) and one having a negative α creates a negative lift (the initial conditions depicted in Figures 11 and 12). A yaw dependence of this type is characteristic of an odd-power series in α. For small yaw, the expansion can be truncated after the first power in α:

$$C_L = C_{l_\alpha} \alpha , \tag{7}$$

where C_{l_α} is the derivative of the lift coefficient with respect to α.

Suppose the original line of fire is defined to be the z axis and that gravity and the Coriolis force are ignored. Furthermore, assume the cg motion is 2-D planar, in particular, assume the motion is confined to the vertical plane, then $\vec{u} = \dot{z}\hat{z} + \dot{y}\hat{y}$ (where a dot indicates time differentiation), as shown in Figure 13.

17
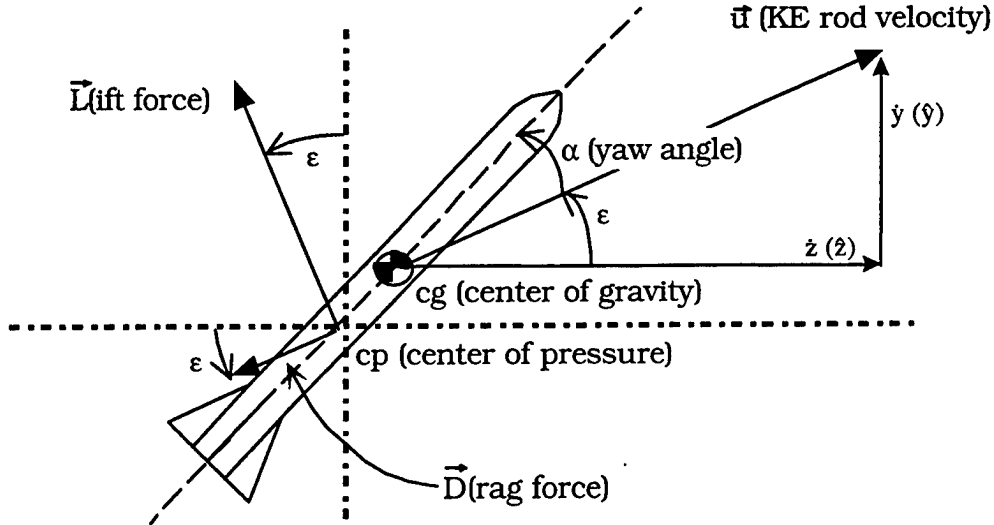
Figure 13. Illustration of 2-D Planar Force and Velocity Components.

From Newton's second law for linear motion in the $\hat{y}$ direction,

$$m \frac{d\dot{y}}{dt} = \bar{L} \cdot \hat{y} + \bar{D} \cdot \hat{y} = \frac{\alpha}{|\alpha|} \left\{ |\bar{L}| \cos \varepsilon \right\} - |\bar{D}| \sin \varepsilon \quad , \tag{8}$$

where m is the mass of the projectile and the ratio $\alpha/|\alpha|$ accounts for the positive and negative influence of yaw on lift. The counterclockwise (positive) angular deviation, ε, of $\bar{u}$ from the original line of fire is assumed small; nevertheless, it is not necessary to neglect ε entirely in order to simplify Equation 8. If the coordinate axes $\hat{z}$ and $\hat{y}$ are simply rotated by the angle ε (i.e., the $\tan^{-1}$ of the cg trajectory) at z_1 and y_1, and thereafter denoted $\hat{s}$ and $\hat{Y}$, respectively, as shown in Figure 14, then the equation of motion becomes

$$m \frac{d\dot{Y}(s)}{dt} = \bar{L} \cdot \hat{Y} + \bar{D} \cdot \hat{Y} \approx \frac{\alpha}{|\alpha|} |\bar{L}| \quad , \tag{9}$$

where lift is nearly parallel with, and drag nearly perpendicular to, the Y axis (even though it may not appear this way in the not-to-scale sketch of Figure 14). In this coordinate system, the locus of points Y(s) defines the swerve curve, which oscillates about the swerve axis, $\hat{s}$. Note, $\bar{u}$ will actually oscillate about some average vector; however, the magnitude of this oscillation is small, so that, $\bar{u} (= \dot{z}\hat{z} + \dot{y}\hat{y}) \approx \dot{s}\hat{s}$.

18

(Note also, for future reference, if the direction of positive $\hat{y}$ and positive $\hat{Y}$ had been defined as opposite of that assigned here [viz., if $\hat{y}$ and $\hat{Y}$ were defined as positive downward], yet α was still considered positive when the nose of the KE rod is above its cg velocity vector, then the right-hand side of Equations 8 and 9 would change signs. This minus sign would carry through in subsequent equations; ultimately, it would change the sign of the final expression for AJ. In other words, as stated in the kinematical discussion of AJ, the sign convention for positive transverse displacement will affect the sign convention for AJ.)

Simply stated, Equation 9 establishes that lift is the primary cause of swerve, and, from Equations 6 and 7, lift is proportional to yaw; hence

$$ m \frac{d\dot{Y}(s)}{dt} = \frac{\alpha}{|\alpha|} \left| \frac{1}{2} \rho A |\bar{u}|^2 C_{l_\alpha} \alpha \right| = \frac{1}{2} \rho A |\bar{u}|^2 C_{l_\alpha} \alpha \quad . \tag{10} $$
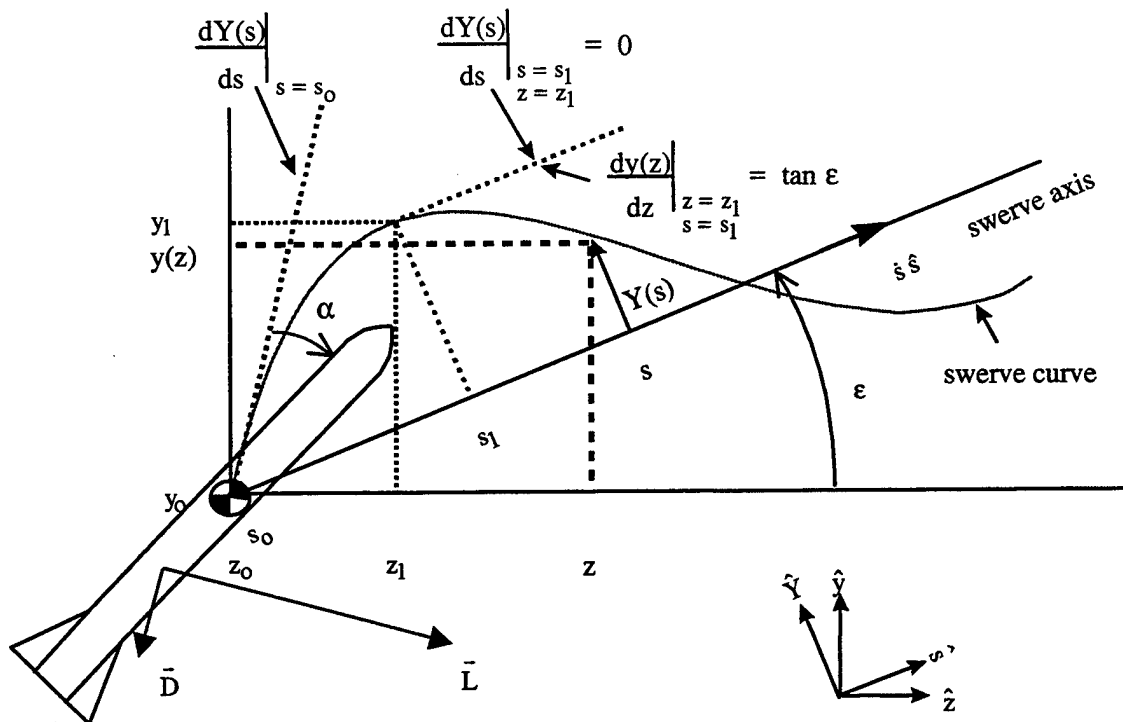

Figure 14. Swerve-Fixed ($\hat{s}, \hat{Y}$) and Earth-Fixed ($\hat{z}, \hat{y}$) Coordinate System (Illustrated Dimensions are Not to Scale).

The expression for α must satisfy the torque equation, viz.,

$$m\,k^2\,\frac{d\dot{\alpha}}{dt}\,(-\hat{x}) = \bar{M} \quad , \tag{11}$$

where k^2 is the radius of gyration of the KE rod about its transverse (x) axis. Furthermore, in accordance with the right-hand rule, a counterclockwise angular acceleration of the rod (relative to the positive-s(werve) axis) must be represented by a negative-x directed vector (which points out of the page), hence, the negative unit vector, $-\hat{x}$, appears in Equation 11.

In FF, the axis of the projectile will oscillate about its cg trajectory (i.e., the z, y or s, Y curve, depending on the coordinate system chosen). Just as air opposes the forward motion of the projectile, it will also oppose this oscillating motion. Hence, there will be a resisting torque, known as the damping moment, that varies with the yaw rate. As the name implies, the damping moment causes the yaw magnitude to diminish with time of flight. However, since it has been argued in the previous illustrations that $\angle AJ$ is established within a relatively short segment of the trajectory, the effect of damping on AJ can be ignored. In this case, the moment $\bar{M}$ about the cg will only be due to the resultant force, $\bar{R} = \bar{L} + \bar{D}$, located at the center of pressure, cp (Figure 13). Thus,

$$\bar{M} = \left|cg - cp\right|\left(\left|\bar{D}\right|\sin\alpha + \frac{\alpha}{|\alpha|}\left|\bar{L}\right|\cos\alpha \right)\hat{x}$$

$$\approx \left|cg - cp\right|\left(\left|\bar{D}\right|\alpha + \frac{\alpha}{|\alpha|}\left|\bar{L}\right| \right)\hat{x} \tag{12}$$

for small α (e.g., < 5°). Note, a positive α will generate a positive-x directed $\bar{M}$.

Using Equations 5–7 in Equation 12, yields

$$\bar{M} = \frac{1}{2} \rho A |\bar{u}|^2 |cg - cp| \alpha \left(C_D + C_{l_\alpha}\right) \hat{x}$$

$$= - \frac{1}{2} C_{m_\alpha} \rho A |\bar{u}|^2 \, d\alpha \, \hat{x} \tag{13}$$

where $C_{m_\alpha} \left(\equiv - \left[C_D + C_{l_\alpha} \right] |cg - cp| \middle/ d \right)$ is called the derivative of the restoring (overturning, or pitching) moment coefficient with respect to α, and d is the rod diameter. By definition, C_{m_α} is negative for a statically stable projectile. The coefficients C_D, C_{l_α}, and C_{m_α} can all be determined from wind-tunnel measurements, or, they can be numerically predicted using computational fluid dynamics (CFD).

Substituting Equation 13 into Equation 11 produces

$$m k^2 \frac{d\dot{\alpha}}{dt} = \frac{1}{2} C_{m_\alpha} \rho A |\bar{u}|^2 \, d\alpha \quad . \tag{14}$$

Since C_{m_α} is negative for the KE projectile, this differential equation for α is of the form $\ddot{\alpha} \propto -\alpha$. Such an equation has a sinusoidal solution, which then means Y(s), from Equation 10, will have a sinusoidal solution (however, α and Y will be 180° out of phase). It is now proven that this oscillatory motion, coupled with the lift force, can account for AJ.

5. A MATHEMATICAL FORMULATION FOR AJ

It was stated in the kinematical discussion of section 2 (viz., Equation 3) that an alternative definition for $\angle$AJ can be defined as:

$$\angle \text{AJ} = \tan^{-1}\left\{\left.\frac{dy}{dz}\right|_{z_1}\right\} - \tan^{-1}\left\{\left.\frac{dy}{dz}\right|_{z_0}\right\} \approx \left.\frac{dy}{dz}\right|_{z_1} - \left.\frac{dy}{dz}\right|_{z_0}$$

, (15)

$$\left(= \left.\frac{\dot{y}}{\dot{z}}\right|_{z_1} - \left.\frac{\dot{y}}{\dot{z}}\right|_{z_0} \approx \frac{\dot{y}(z_1) - \dot{y}(z_0)}{\dot{z}}\right)$$

where, it will be recalled, z_1 is taken to be the downrange coordinate of the first local swerve maxima (relative to the swerve axis), while z_0 is the designation for the downrange coordinate at the origin of FF (cf., Figures 8 and 14). Hence, from Equation 15, $\angle \text{AJ}$ can be viewed as a <u>change</u> in slope of the cg trajectory from z_0 to z_1 (or, it can be viewed as a <u>change</u> in transverse velocity from z_0 to z_1, nondimensionalized by the longitudinal velocity [assumed to be constant from z_0 to z_1]).

Equation 3 (and 15) defines $\angle \text{AJ}$ in terms of dy/dz; to find its equivalent expression in terms of dY/ds, it is necessary to find the transformation algorithm between y and Y, and z and s. To that end (with the aid of Figure 14), it can be shown that

$$y(z) = Y(s) \cos \varepsilon + (s - s_0) \sin \varepsilon$$
. (16)
$$z = (s - s_0) \cos \varepsilon - Y(s) \sin \varepsilon$$

From Equation 16,

$$\frac{dy(z)}{dz} = \frac{\dfrac{dy(z)}{ds}}{\dfrac{dz}{ds}} = \frac{\dfrac{dY(s)}{ds} \cos \varepsilon + \sin \varepsilon}{\cos \varepsilon - \dfrac{dY(s)}{ds} \sin \varepsilon}$$

. (17)

$$\approx \frac{dY(s)}{ds} + \tan \varepsilon \quad , \quad \text{for } \frac{dY(s)}{ds}, \varepsilon \ll 1$$

Hence, from Equations 15 and 17,

$$\angle AJ \;=\; \left.\frac{dy}{dz}\right|_{z_1,\,s_1} \;-\; \left.\frac{dy}{dz}\right|_{z_0,\,s_0} \;=\; \left.\frac{dY}{ds}\right|_{s_1,\,z_1} \;-\; \left.\frac{dY}{ds}\right|_{s_0,\,z_0}$$

$$\left(\;=\; \left.\frac{\dot{Y}}{\dot{s}}\right|_{s_1} \;-\; \left.\frac{\dot{Y}}{\dot{s}}\right|_{s_0} \;\approx\; \frac{\dot{Y}(s_1) - \dot{Y}(s_0)}{|\bar{u}|}\;\right), \qquad (18)$$

where the subscript notation z_1, s_1 (for example) refers to the point on the swerve curve with coordinate z_1 along the z axis and s_1 along the s axis (cf. Figure 14), and time and space derivatives are related by

$$\dot{Y} \;\equiv\; \frac{dY}{dt} \;=\; \frac{dY}{ds}\frac{ds}{dt} \;=\; |\bar{u}|\,\frac{dY}{ds} \quad . \qquad (19)$$

In effect, Equation 18 states the obvious—the difference in slopes between two points on the swerve curve does not change if the coordinate system, used to describe the curve, is rotated through an angle ε (this fact is also acknowledged in Appendix A).

Combining Equations 9, 10 and 14, it can be shown that

$$d\dot{Y} \;=\; \frac{\left(\bar{L}\cdot\hat{Y}\right)dt}{m} \;=\; \frac{C_{l_\alpha}k^2}{d\,C_{m_\alpha}}\,d\dot{\alpha} \quad . \qquad (20)$$

Denoting $\dot{\alpha}_0$ and s_0 as the initial conditions at entry into FF and $\dot{\alpha}_1$ and s_1 as the conditions at the first local maximum in the swerve curve, then integration of Equation 20 yields

$$\dot{Y}(s_1) - \dot{Y}(s_0) \;=\; \int_{\dot{Y}(s_0)}^{\dot{Y}(s_1)} d\dot{Y} \;=\; \frac{1}{m}\int_{t(s_0)}^{t(s_1)}\left(\bar{L}\cdot\hat{Y}\right)dt$$

$$=\; \int_{\dot{\alpha}_0}^{\dot{\alpha}_1}\frac{C_{l_\alpha}k^2}{d\,C_{m_\alpha}}\,d\dot{\alpha} \;=\; \frac{C_{l_\alpha}k^2}{d\,C_{m_\alpha}}\left(\dot{\alpha}_1 - \dot{\alpha}_0\right) \qquad (21)$$

Combining Equations 18 and 21, yields

$$\angle AJ = \frac{dY}{ds}\bigg|_{s_1, z_1} - \frac{dY}{ds}\bigg|_{s_0, z_0}$$ (22)

$$\approx \frac{1}{m|\bar{u}|} \int_{t(s_0)}^{t(s_1)} \left(\bar{L} \cdot \hat{Y} \right) dt = \frac{C_{l_\alpha} k^2}{d\, C_{m_\alpha} |\bar{u}|} \left(\dot{\alpha}_1 - \dot{\alpha}_0 \right)$$

Equation 18 shows that $\angle AJ$ can be viewed as a <u>change</u> in the slope of the cg trajectory (or equivalently, a change in the ratio of the transverse swerve velocity to the longitudinal swerve velocity) from z_0 (s_0) to z_1 (s_1). Equation 22 shows that $\angle AJ$ can also be related to a <u>change</u> in angular rates from z_0 (s_0) to z_1 (s_1). Furthermore, the insertion of the lift correlation in Equation 20 and its retention in Equations 21 and 22 serves to underscore the physical explanation given in section three of this report, viz., that $\angle AJ$ is due to the (integrated) effect of lift, caused by yaw, from z_0 (s_0) to z_1 (s_1).

Note, Equations 18, 21, and 22 could have been simplified by setting $dY/ds\big|_{s_1, z_1} = 0$ and $\dot{Y}(s_1) = 0$, since, by definition, $Y(s)$ is at a local maxima at s_1, z_1. (This would also mean [from Equation 17] that $dy/dz\big|_{z_1, s_1} = \tan \varepsilon$, as marked in Figure 14.) Moreover, since α and Y are $180°$ out of phase, when $\dot{Y}(s_1) = 0$, $\dot{\alpha}_1 = 0$; hence, Equation 22 can be simplified to:

$$\angle AJ = -\frac{dY}{ds}\bigg|_{s_0, z_0} = -\frac{C_{l_\alpha} k^2}{d\, C_{m_\alpha} |\bar{u}|} \dot{\alpha}_0$$ (23)

From Equation 22, it can be seen that $\angle AJ$ will increase if either the integrand (viz., the lift force) or the domain of integration (viz. the lift force action time) increases. In more fundamental terms (noting that C_{m_α} will

24

always be negative for a KE rod, and C_{l_α}, k, d, and $|\bar{u}|$ are all positive), $\angle AJ$ will increase if either 1) C_{l_α} increases (so that the lifting force per degree yaw increases), 2) k increases (in which case, the rod would rotate slower, and hence the lifting force would act longer), 3) $\dot{\alpha}_o$ increases (so that, once again, it would take more time to bring the rod to rest), or 4) C_{m_α} decreases (so that the overturning moment per degree yaw decreases, again lengthening the action time for the lifting force).

Other, equivalent expressions for AJ that can be found in the literature include:

$$\angle AJ = -(+)\frac{C_{l_\alpha} k^2}{d\, C_{m_\alpha} |\bar{u}|} \dot{\alpha}_o \equiv -(+)\frac{C_{l_\alpha} I_t}{m |\bar{u}| d\, C_{m_\alpha}} \dot{\alpha}_o \equiv -(+)\frac{C_{l_\alpha} I_t}{m\, d^2\, C_{m_\alpha}} \alpha'_o \quad , (24)$$

where I_t (= mk^2) is the moment of inertia of the (symmetric) projectile about its transverse axis, and α'_o is the initial FF rate of change of yaw with respect to the trajectory arc length, measured in rod diameters (i.e., $\alpha'_o \equiv d\alpha / d[s/d] \,|_{s_o, z_o}$).

Depending on the coordinate system used, there may or may not be a negative sign on the right-hand side in the equalities/identities of Equation 24. The convention chosen here is to define both the positive vertical axis (y) and positive yaw (α) as up (up for α means its nose is above the cg velocity vector). However, it is more common in the field ballistics to define the positive vertical axis as down, and positive yaw as up; in this case, the negative sign convention is absent in Equation 24 (thereby explaining the plus signs in parentheses). The plus-sign form of the expression for $\angle AJ$ is, by far, the most common construction (e.g., Murphy and Bradley [1959], Murphy [1963], Fansler and Schmidt [1975], Schmidt [1996]). There is one other sign variation that may appear in the literature; if both the positive vertical axis and positive yaw are defined as down, then the sign remains

25

negative in Equation 24 (e.g., Murphy [1957], Lijewski [1982]). Regardless of the sign convention for the coordinate system used, it is always the case, as Murphy and Bradley (1959) state, that "jump due to α'_0 is in the direction of α'_0."

6. CONCLUSIONS AND COMMENTARY

Equation 3 (or 15) provides a "limitless" kinematical definition for $\angle AJ$, which, reassuringly, leads to the traditional dynamical expression for $\angle AJ$, viz. Equation 24. The origins of possible variations in the sign convention of Equation 24 were explored, but the primary objective of this report was to answer the questions: what is AJ, what does it mean, and what aspect of the flight trajectory does it refer to, or account for.

For instance, one misconception about AJ seems to arise from the fact that Equation 24 only shows a dependence on the initial yaw rate at the origin of FF (concealing the fact that it is actually a difference in rates [Equation 22] that happens to equal the initial rate [Equation 23]). Therefore, some may conclude from this (apparent) point dependence that AJ is a "point-based" phenomenon, i.e., that it results from (aero)dynamical effects that occur at the origin of FF. Others, seeking a geometrical explanation for AJ, may forgo the dynamical definition of Equation 24 and return to its origin in the kinematical definition, adopted, for example, by Murphy (1957) or Murphy (1963). However, those geometry-based definitions for AJ (Equations 1. or 2) call for the cg coordinates to be evaluated in the limit of an infinite trajectory. There is some risk that those drawing upon this definition to explain AJ will erroneously assume that it is a transformation that accumulates with downrange distance (not realizing that the swerve axis is actually a constant, established long before the trajectory reaches infinity).

26

The central theme of this report is to show that AJ is neither a change in direction that takes place at a point, nor is it a curving change that takes place over a domain of infinite extent, but rather, it is a regional transformation. In particular, using an alternative kinematic definition, it was illustrated geometrically (in terms of the cg trajectory), argued physically (in terms of yaw and lift), and proven mathematically (based on Newton's equations of motion), that $\angle$AJ for a (nonspinning) KE penetrator can be accounted for by the change in transverse cg velocity—due to lift—acting for the short period of time and space from entry of the projectile into FF until it reaches its first local maxima in yaw (or swerve).

7. REFERENCES

Bornstein, J., I. Celmins, P. Plostins, and E. M. Schmidt. "Techniques for the Measurement of Tank Cannon Jump." BRL-MR-3715, U.S. Army Ballistic Research Laboratory, Aberdeen Proving Ground, MD, December 1988.

Fansler, K. S., and E. M. Schmidt. "The Influence of Muzzle Gasdynamics Upon the Trajectory of Fin-Stabilized Projectiles." BRL-R-1793, U.S. Army Ballistic Research Laboratory, Aberdeen Proving Ground, MD, June 1975.

Lijewski, L. E. "Aerodynamic Jump Prediction for Supersonic, High Fineness Ratio, Cruciform Finned Bodies." *Journal of Guidance, American Institute of Aeronautics and Astronautics*, vol. 5, no. 5, pp. 521–528, September–October 1982.

Murphy, C. H. "Comments on Projectile Jump." BRL-MR-1071, U.S. Army Ballistic Research Laboratories, Aberdeen Proving Ground, MD, April 1957, AD 132323.

Murphy, C. H., and J. W. Bradley. "Jump Due to Aerodynamic Asymmetry of a Missile With Varying Roll Rate." BRL-R-1077, U.S. Army Ballistic

Research Laboratories, Aberdeen Proving Ground, MD, May 1959, AD 219312.

Murphy, C. H. "Free Flight Motion of Symmetric Missiles." BRL-R-1216, U.S. Army Ballistic Research Laboratories, Aberdeen Proving Ground, MD, July 1963.

Schmidt, E. M. "A Technique for Reduction of Launch-Induced Perturbations." *Proceedings of the Eighth U.S. Army Symposium on Gun Dynamics*, ARCCB-SP-96032, U.S. Army Armament Research, Development, and Engineering Center, Benet Laboratories, Watervliet, NY, pp. 12-1–12-7, May 1996.

Appendix A:

Proof: Tangents To The Swerve Maxima Run Parallel To The Swerve Axis

Equation 3 of section 2 gives an alternative kinematical definition for $\angle AJ$. The validity of this alternative definition is based upon the assumption that to tangents to the swerve curve at any of the local maxima (relative to the swerve axis) are parallel to the swerve axis. This appendix supplies the proof that this assumption is indeed true. The proof begins with the special case where the swerve axis is horizontal (it is then generalized to the case where the swerve axis is oriented at any oblique angle with respect to horizontal). To first order in the differential of the downrange (Figure A-1) swerve curve coordinate, z, viz., dz, the transverse swerve curve coordinate, y (at the location of a local swerve maximum, z_{max}), will be given by

$$y(z_{max}) = y(z_{max} - dz) + \left(\frac{dy}{dz} \bigg|_{z_{max} - dz} \right) dz$$

$$(A-1)$$

$$y(z_{max}) = y(z_{max} + dz) - \left(\frac{dy}{dz} \bigg|_{z_{max} + dz} \right) dz$$

Since $y(z_{max})$ is considered to be a local maximum, then

$$y(z_{max}) = y(z_{max} - dz) + \varepsilon$$

$$\varepsilon, \delta > 0 \quad . \qquad (A-2)$$

$$y(z_{max}) = y(z_{max} + dz) + \delta$$

Combining Equations A-1 and A-2,

$$\varepsilon = \left(\frac{dy}{dz} \bigg|_{z_{max} - dz} \right) dz$$

$$(A-3)$$

$$\delta = - \left(\frac{dy}{dz} \bigg|_{z_{max} + dz} \right) dz$$

In which case, since ε, δ and dz are all positive,

$$\left(\left. \frac{dy}{dz} \right|_{z_{max}-dz} \right) > 0$$

A-4

$$\left(\left. \frac{dy}{dz} \right|_{z_{max}+dz} \right) < 0$$

Since the derivatives must be continuous at z_{max},

$$\lim_{dz \to 0} \left(\left. \frac{dy}{dz} \right|_{z_{max}-dz} \right) \to 0^{+}$$

A-5

$$\lim_{dz \to 0} \left(\left. \frac{dy}{dz} \right|_{z_{max}+dz} \right) \to 0^{-}$$

in which case,

$$\left. \frac{dy}{dz} \right|_{z_{max}} = 0 \quad .$$

A-6

If the location of z_{max} had been a local minimum (instead of a local maximum), then ε and δ are < 0 in the above steps, resulting in a reversal of the inequalities; however, the conclusion, Equation A-6, will not change. Hence, it has been shown that the slope of the swerve curve at local maxima (positive or negative) will run parallel with the slope of the swerve axis, for this special case where the swerve axis is coincident with the horizontal axis.

Note, nothing has been stated, thus far, about the particular form that the swerve curve y(z) must have, other than, z_{max} denotes the location of a local maxima in the curve, and the fact that the curve must have continuous first derivatives at z_{max}. Both of these generic requirements are satisfied by a damped sine wave, used to approximate the swerve curve (in each of the two transverse planes) for a nonspinning KE rod. For reference, Figure A-1 shows

31

both a sine waveform and a damped sine waveform, with wavelength λ, amplitude A, and decay constant γ. The slopes indicated by Equations A-4 and A-6 are portrayed on each waveform at a local maxima. Also shown in the inset of Figure A-1 is the physical rotation (through some acute angle) of the coordinate axis and its accompanying swerve curves. Rotating the coordinate system rotates the swerve curve axis and all points on the swerve curve, along with their tangents. As far as its effect on the reorientation of the swerve curve, rotation of the coordinate system is tantamount to rotation of just the swerve curve in a fixed coordinate system. From the principles of geometry, any rotation of a figure (or curve) can be decomposed into two reflections ("two-reflection theorem"), and reflection transformations are known to preserve angles ("reflection postulate"). Hence, if the tangent lines at local swerve maxima run parallel with the swerve axis in the special case, where the swerve axis is coincident with the horizontal axis (Equations A-1 – A-6), then these tangent lines will remain parallel with the swerve axis when the swerve curve is rotated. This completes the proof of this appendix.
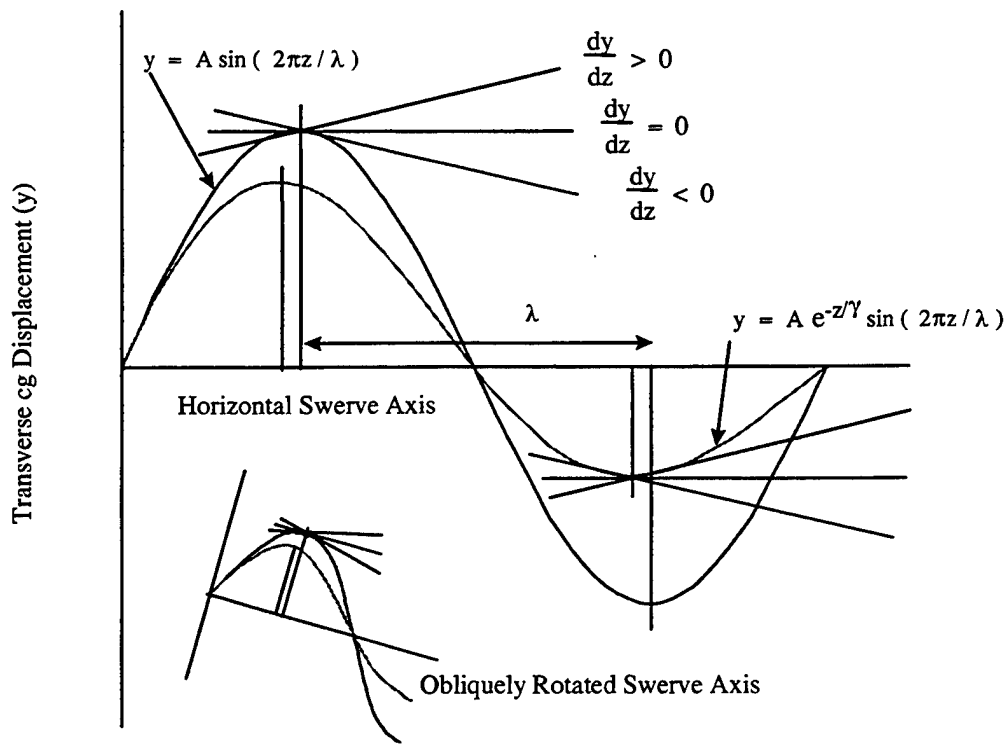
Figure A-1. 2-D Planar Waveforms, Their Tangents at Local Maxima And Their Rotational Congruencies.

32

APPENDIX B:

PHASE RELATIONSHIPS BETWEEN AERODYNAMIC VARIABLES

Several observations can be made if the development that stopped with Equation 14 is taken one step further. In particular, solving Equation 14, it can be shown that

$$\alpha = \alpha_{max}\cos\left(\omega\,t + \phi\right) = \alpha_{max}\cos\left(\frac{2\pi}{\lambda}\,[\,z - z_o\,] + \phi\right),\qquad (B\text{-}1)$$

where ω is the frequency, t is the time of FF, ϕ is a phase angle at t = 0, λ is the wavelength, and z is the downrange coordinate at time t. Furthermore,

$$\tan\phi = \frac{-\lambda}{2\pi\,|\bar{u}|}\,\frac{\dot{\alpha}_o}{\alpha_o}\;,\quad \alpha_{max} = \sqrt{\alpha_o^2 + \frac{\dot{\alpha}_o^2\,\lambda^2}{(2\pi\,|\bar{u}|)^2}}\;,\quad \lambda = 2\pi\sqrt{\frac{2\,m\,k^2}{\rho\,A\,d\,\left|C_{m_\alpha}\right|}}\;.\ (B\text{-}2)$$

As before, it is assumed here that $z - z_o = |\bar{u}|\,t$ over the short region of interest.

With Equations B-1 and B-2 in hand, a number of additional comments can be made. First, as claimed with Equation 14, it can be seen that α varies periodically in time and space. Even though the relationships between α, $\dot{\alpha}$, y, and $\dot{y}$ are unambiguously defined by the differential equations cited in section 4, their relative behavior is sometimes contrary to first intuition, and for this reason deserves further comment.

A solution for Y(s) is obtained by substituting Equation B-1 into Equation 10 and integrating. This solution is sinusoidal in nature but 180° out of phase with α; likewise $\dot{Y}$ is 180° out of phase with $\dot{\alpha}$.

Figure B-1 illustrates the cyclic nature of various linear and angular motion variables for the special case where the swerve axis is horizontal, so that $y(z) \equiv Y(s \equiv z)$ (in the notation of section 4). For ease of illustration, special initial conditions for the origin of FF are assumed in Figure B-1, viz., $\alpha_o = y_o = 0$, and $\dot{\alpha}_o > 0$, while $\dot{y}_o < 0$.

Describing the motion in Figure B-1, it can be said that at time zero (the origin FF) the projectile will begin to nose up, generating a positive (up) lift force. Since the yaw angle and the lift are both positive in the first half cycle of Figure B-1, it might be assumed that the projectile would continuously move upward during this time interval (or distance). However, as depicted by the y motion curve, this is not the case. What actually happens can be understood, physically, as follows.

Even though the yaw and lift are positive over the first quarter cycle in Figure B-1, the transverse velocity, $\dot{y}$, is initially negative, i.e., the projectile enters FF moving downward (due, for instance, to LD effects). Thus, the work done by positive lift in the first quarter cycle is expended on slowing the downward motion to zero. Only during the second quarter cycle has the lift force acted long enough to reverse the projectile velocity and thus create the positive displacement that may have been erroneously perceived from the onset.
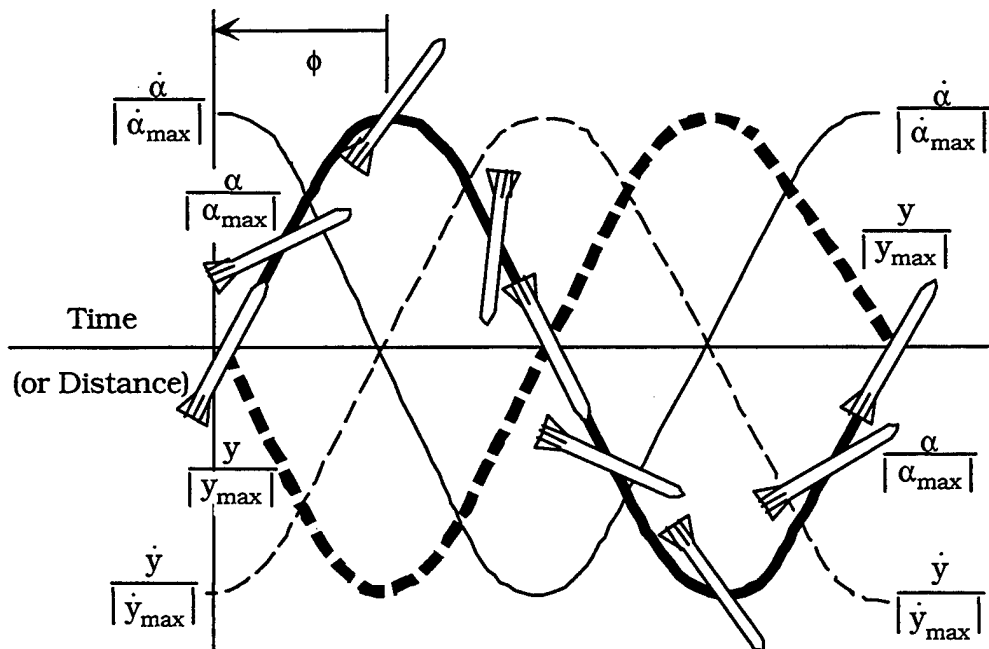
Figure B-1. Illustration of the Phase Relationships Between Transverse and Angular Projectile Variables (Note α and Y are 180° Out of Phase).

35

In view of the possible misconceptions that can arise between yaw and displacement, a common-sense check on the sign of Equation 24 for $\angle AJ$ is in order. Suppose a KE rod enters FF as portrayed in Figure B-1, with $\alpha_o = 0$ ($\phi = -\pi/2$) and $\dot{\alpha}_o > 0$, this would mean the yaw angle is constantly increasing until it reaches its first maximum yaw, α_{max}, where $\dot{\alpha} = 0$. The lift on the nose-up projectile would increase the transverse velocity $\dot{y}$ during this time period (from the negative value it starts with, up to zero), and hence a counterclockwise (positive) $\angle AJ$ is expected. Indeed, this is consistent with the sign generated by Equation 24 when $\dot{\alpha}_o > 0$ and C_{m_α} is negative.

NO. OF COPIES	ORGANIZATION
1	PRIN DPTY FOR TCHNLGY HQ US ARMY MATCOM AMCDCG T M FISETTE AMCDCG A D ADAMS 5001 EISENHOWER AVE ALEXANDRIA VA 22333-0001
1	DPTY ASSIST SCY FOR R&T SARD TT T KILLION THE PENTAGON WASHINGTON DC 20310-0103
1	DUSD SPACE 1E765 J G MCNEFF 3900 DEFENSE PENTAGON WASHINGTON DC 20301-3900
1	USAASA MOAS AI W PARRON 9325 GUNSTON RD STE N319 FT BELVOIR VA 22060-5582
1	DIRECTOR US ARMY RESEARCH LAB AMSRL CS AL TA 2800 POWDER MILL RD ADELPHI MD 20783-1145
4	COMMANDER US ARMY ARMOR CENTER ATSB CD ATSB SBE ORSA FT KNOX KY 40121
2	PEO FOR ARMAMENTS SFAE AR SFAE AR D PICATINNY ARSENAL NJ 07806-5000
1	US ARMY MATERIEL CMD AMCICP AD M FISETTE 5001 EISENHOWER AVE ALEXANDRIA VA 22333-0001
1	US ARMY BMDS CMD ADVANCED TECHLGY CTR PO BOX 1500 HUNTSVILLE AL 35807-3801

NO. OF COPIES	ORGANIZATION
7	CDR TMAS SFAE AR TMA V ROSAMILIA R BILLINGTON W KATZ R JOINSON C ROLLER E KOPACZ K RUBEN PICATINNY ARSENAL NJ 07806-5000
5	CDR US ARMY ARDEC AMSTA AR AE AMSTA AR FSF GD K PFLEGER AMSTA AR FSF BV V GALGANO C GONZALES C LANGEN PICATINNY ARSENAL NJ 07806-5000
1	CDR US ARMY ARDEC AMSTA AR AEE B S BERNSTEIN PICATINNY ARSENAL NJ 07806-5000
5	CDR US ARMY ARDEC AMSTA AR CCH V C MANDALA E FENNELL A GOWARTY J PETTY P VALENTI PICATINNY ARSENAL NJ 07806-5000
4	CDR US ARMY ARDEC AMSTA AR QAT A L DULISSI C PATEL R ROESER G MAGISTRO PICATINNY ARSENAL NJ 07806-5000

NO. OF COPIES	ORGANIZATION	NO. OF COPIES	ORGANIZATION
2	PM AFAS SFAE ASM AF LTC A ELLIS LTC B ELLIS PICATINNY ARSENAL NJ 07806-5000	1	CDR US ARMY TACOM AMSTA JSK S GOODMAN WARREN MI 48397-5000
3	OFFICE OF THE PM M109/AG PALADIN SFAE AR HIP J CARBONE K HURBAN S WALL PICATINNY ARSENAL NJ 07806-5000	1	COMMANDANT US ARMY CMD & GEN STAFF COLLEGE FT LEAVENWORTH KS 66027
		1	COMMANDANT US ARMY SPCL WARFARE SCHL REV AND TRNG LIT DIV FT BRAGG NC 28307
16	DIR US ARMY ARDEC AMSTA AR CCB J KEHN J BATTAGLIA J VASILAKIS G PFLEGL G FRIAR G O'HARA M WITHERELL E KATHE D MOAK R GAST C A ANDRADE J HAAS A GABRIELE P VOTTIS R HASENBEIN S SOPOK BENET LABS WATERVLIET NY 12189	1	COMMANDER RADFORD ARMY AMMO PLANT AMSTE QA HI LIB RADFORD VA 24141-0298
		1	CDR US ARMY NGIC IANG TMT B BEITER 220 SEVENTH STREET NE CHARLOTTESVILLE VA 22902-5396
		1	COMMANDANT US ARMY ARMOR SCHOOL ATZK CD MS M FALKOVITCH ARMOR AGENCY FT KNOX KY 40121-5215
		1	CDR US ARMY TRADOC DIR OF TRNG & DOCTRINE DEVELOPMENT DOCTRINE DIVISION ATZK TDD G MR POMEY FT KNOX KY 40121-5000
1	PM US ARMY TACOM AMCPM ABMS T DEAN WARREN MI 48092-2498		
1	CDR US ARMY TACOM SFAE ASM AB SW DR PATTISON WARREN MI 48397-5000	1	COMMANDER USA ARMAMENTS MUNITIONS & CHEMICAL CMD AMSMC DSD C J O'DONNELL ROCK ISLAND IL 61299-6000
1	CDR US ARMY TACOM ABRAMS TANK SYSTEM SFAE ASM AB WARREN MI 48397-5000	2	PROJECT MANAGER SADARM PICATINNY ARSENAL NJ 07806-5000

NO. OF COPIES	ORGANIZATION
7	PM TMAS SFAE AR TMA COL R PAWLICK K KIMKER D GUZIEWICZ C CORDING SFAE AR TMA MD R KOWALSKI J WILSON B DACEY PICATINNY ARSENAL NJ 07806-5000
3	PEO FIELD ART SYS SFAE FAS PM D ADAMS T MCWILLIAMS H GOLDMAN PICATINNY ARSENAL NJ 07806-5000
2	PM AFAS G DELCOCO J SHIELDS PICATINNY ARSENAL NJ 07806-5000
3	HQDA SARD TR R CHAITT MS K KOMINOS SARD TT F MILTON PENTAGON WASHINGTON DC 20310-0103
1	COMMANDER SMCWV QAE Q C HOWD BLDG 44 WATERVLIET ARSNL WATERVLIET NY 12189-4050
1	COMMANDER SMCWV SPM T MCCLOSKEY BLDG 25 3 WATERVLIET ARSNL WATERVLIET NY 12189-4050
1	COMMANDER WATERVLIET ARSENAL SMCWV QA QS K INSCO WATERVLIET NY 12189-4050

NO. OF COPIES	ORGANIZATION
1	COMMANDER US ARMY BELVOIR RD&E CTR STRBE JBC FT BELVOIR VA 22060-5606
1	DIR USARL AMSRL WT L D WOODBURY 2800 POWDER MILL RD ADELPHI MD 20783-1145
2	US ARMY RESEARCH OFFICE A CROWSON J CHANDRA PO BOX 12211 RESEARCH TRIANGLE PARK NC 27709-2211
3	US ARMY RESEARCH OFFICE R SINGLETON G ANDERSON K IYER ENGINEERING SCIENCES DIV PO BOX 12211 RESEARCH TRIANGLE PARK NC 27709-2211
4	COMMANDER US ARMY MISSILE COMMAND AMSMI RD W MCCORKLE AMSMI RD W G SNYDER AMSMI RD ST P DOYLE AMSMI RD ST CN T VANDIVER REDSTONE ARSENAL AL 35898
1	SDIO TNI L H CAVENY PENTAGON WASHINGTON DC 20301-7100
1	SDIO DA E GERRY PENTAGON WASHINGTON DC 21301-7100

NO. OF COPIES	ORGANIZATION	NO. OF COPIES	ORGANIZATION
4	CDR NAVAL RSRCH LAB TECHNICAL LIBRARY CODE 4410 K KAILASANATE J BORIS E ORAN WASHINGTON DC 20375-5000	1	CDR NSWC CODE G33 J FRAYSSE CODE D4 M E LACY 17320 DAHLGREN RD DAHLGREN VA 22448-5000
1	OFFICE OF NAVAL RSRCH CODE 473 R S MILLER 800 N QUINCY ST ARLINGTON VA 22217-5000	2	COMMANDER NAVAL AIR WARFARE CTR CODE 388 C F PRICE T BOGGS CHINA LAKE CA 93555-6001
1	OFFICE OF NAVAL TECHLGY ONT 213 D SIEGEL 800 N QUINCY ST ARLINGTON VA 22217-5000	2	COMMANDER NAVAL AIR WARFARE CTR CODE 3895 T PARR R DERR CHINA LAKE CA 93555-6001
1	CDR NSWC CODE 730 SILVER SPRING MD 20903-5000	1	COMMANDER NAVAL AIR WARFARE CTR INFORMATION SCIENCE DIV CHINA LAKE CA 93555-6001
1	CDR NSWC CODE 13 R BERNECKER SILVER SPRING MD 20903-5000	1	OFFICE OF NAVAL RESEARCH Y RAJAPAKSE MECH DIV CODE 1132SM ARLINGTON VA 22217
7	CDR NSWC T C SMITH K RICE S MITCHELL S PETERS J CONSAGA C GOTZMER TECH LAB INDIAN HEAD MD 20640-5000	1	NAVAL ORDNANCE STATION D HOLMES CODE 2011 ADVANCED SYS TECH BR LOUISVILLE KY 40214-5245
4	CDR NSWC CODE G30 GUNS & MUNITIONS DIV CODE G32 GUNS SYS DIV CODE G33 T DORAN CODE E23 TECH LIB DAHLGREN VA 22448-5000	1	EXPED WARF DIV N85 F SHOUP 2000 NAVY PENTAGON WASHINGTON DC 20350-2000
3	CDR NSWC CODE G33 (2 CPS) CODE G30 J H FRANCIS DAHLGREN DIV DAHLGREN VA 22448-5000	1	COMMANDER NAVAL SEA SYSTEMS CMD D LIESE 2531 JEFFERSON DAVIS HWY ARLINGTON VA 22242-5160
		1	GPS JOINT PROG OFC DIR COL J CLAY 2435 VELA WAY STE 1613 LOS ANGELES AFB CA 90245-5500

44

NO. OF COPIES	ORGANIZATION	NO. OF COPIES	ORGANIZATION
3	THIOKOL CORPORATION R WILLER R BIDDLE TECH LAB ELKTON DIVISION PO BOX 241 ELKTON MD 21921-0241	2	UNITED DEFENSE LP P PARA G THOMAS 1107 COLEMAN AVE BOX 367 SAN JOSE CA 95103
3	VERITAY TECHLGY INC E B FISHER A CRICKENBERGER J BARNES PO BOX 305 4845 MILLERSPORT HWY EAST AMHERST NY 14501-0305	1	UNITED DEFENSE B HELD MAIL STOP M387 4800 EAST RIVER RD MINNEAPOLIS MN 55421-1498

ABERDEEN PROVING GROUND

NO. OF COPIES	ORGANIZATION	NO. OF COPIES	ORGANIZATION

1	UNIVERSAL PROPULSION COMPANY
	H J MCSPADDEN
	25401 NORTH CENTRAL AVE
	PHOENIX AZ 85027-7899
		37	DIR USARL
			AMSRL WM B
			  A HORST
			AMSRL WM BC
			  S WILKERSON
			  P PLOSTINS
			  D LYON

1	SRI INTERNATIONAL
	TECH LIB
	PROPULSION SCIENCES DIV
	333 RAVENWOOD AVE
	MENLO PARK CA 94025-3493
			J SAHU
			  M BUNDY (4 CPS)
			  B GUIDOS
			  P WEINACHT
			  K SOENCKSEN
			  A MIKHAIL

1	GENERAL DYNAMICS
	D BARTLE
	LAND SYSTEMS DIVISION
	PO BOX 1901
	WARREN MI 48090
			H EDGE
			  A ZIELINSKI
			  D WEBB
			  G COOPER
			  J NEWILL
			  J GARNER

1	PM ADVANCED CONCEPTS
	R TAYLOR
	LORAL VOUGHT SYSTEMS
	PO BOX 650003 MS WT 21
	DALLAS TX 76265-0003
			T ERLINE
			  V OSKAY
			  C RUTH
			AMSRL WM MB
			  B BURNS
			  L BURTON
			  W DRYSDALE

2	LORAL VOUGHT SYSTEMS
	G JACKSON
	K COOK
	1701 W MARSHALL DR
	GRAND PRAIRIE TX 75051
			AMSRL WM BP
			  E SCHMIDT
			AMSRL WM BA
			  W D'AMICO
			  F BRANDON
			  B DAVIS
			  M HOLLIS

4	GEN DYNAMICS ARMAMENT SYS
	G CROMACK
	J TALLEY
	LAKESIDE AVE
	BURLINGTON VT 05401-4985
			AMSRL WM BB
			  T VONG
			  J WALL
			  R YALAMANCHILI

NO. OF
COPIES ORGANIZATION

         AMSRL WM BE
           G WREN
           W OBERLE
           G KATULKA
           M NUSCA

USER EVALUATION SHEET/CHANGE OF ADDRESS

This Laboratory undertakes a continuing effort to improve the quality of the reports it publishes. Your comments/answers to the items/questions below will aid us in our efforts.

1. ARL Report Number/Author_____ARL-TR-1872 (Bundy)_____ Date of Report __January 1999_____

2. Date Report Received _____

3. Does this report satisfy a need? (Comment on purpose, related project, or other area of interest for which the report will be used.) _____

_____

_____

4. Specifically, how is the report being used? (Information source, design data, procedure, source of ideas, etc.) _____

_____

_____

5. Has the information in this report led to any quantitative savings as far as man-hours or dollars saved, operating costs avoided, or efficiencies achieved, etc? If so, please elaborate. _____

_____

_____

6. General Comments. What do you think should be changed to improve future reports? (Indicate changes to organization, technical content, format, etc.) _____

_____

_____

_____

CURRENT
ADDRESS

Organization _____

Name _____ E-mail Name _____

Street or P.O. Box No. _____

City, State, Zip Code _____

7. If indicating a Change of Address or Address Correction, please provide the Current or Correct address above and the Old or Incorrect address below.

OLD
ADDRESS

Organization _____

Name _____

Street or P.O. Box No. _____

City, State, Zip Code _____

(Remove this sheet, fold as indicated, tape closed, and mail.)
(DO NOT STAPLE)

DEPARTMENT OF THE ARMY

OFFICIAL BUSINESS

BUSINESS REPLY MAIL
FIRST CLASS PERMIT NO 0001,APG,MD

POSTAGE WILL BE PAID BY ADDRESSEE

DIRECTOR
US ARMY RESEARCH LABORATORY
ATTN AMSRL WM BC
ABERDEEN PROVING GROUND MD 21005-5066